Axel and T. Maniatis, Eds. (Academic Press, New York, 1979), vol. 14, p. 57.
38. The polyacrylamide slab gel (1.27 mm by 9 cm by 14 cm) of 12.5 percent acrylamide (*39*) containing 8*M* urea (*20, 21*) was washed for 30 minutes in two changes of phosphate-buffered saline (PBS) solution. The gel was placed on CNBr-activated filter paper (*40*) for 1 hour at room temperature, and the gel was later stained with Coomassie brilliant blue. The paper was treated in PBS containing 0.1*M* glycine and 0.2 percent bovine serum albumin (BSA) at 37°C for 4 hours (or 18 hours at 4°C), washed in PBS for 10 minutes, placed in a plastic bag, and treated for 1 hour at 37°C with 5 percent guinea pig serum in PBS (GPS-PBS) followed by (7.5×10^6 to 10×10^6 cpm) ^{125}I-labeled guinea pig immunoglobulin G (IgG) specific for VP_3 in 10 ml of GPS-PBS. The VP_3-specific antibody was iodinated [100 μg of IgG, 10 μg of Iodogen (Pierce), and 500 μCi of ^{125}I (NaI) for 15 minutes at room temperature] and separated by G-25 Sephadex chromatography. After 4 hours at room temperature, the filter paper was washed with 30 ml of GPS-PBS for 1 hour, rinsed twice with 200 ml of PBS for 18 hours, blotted, air-dried, and exposed to x-ray film with the use of an intensifying screen at −60°C.
39. J. V. Maizel, *Methods Virol.* **5**, 177 (1971).
40. R. Hitzeman, L. Clarke, J. Carbon, *J. Biol. Chem.* **225**, 12073 (1980).
41. We thank Karl Axelson, James Dean, Nicholas Shuot, Marla Koster, and JoAnn Henry of the Plum Island Animal Disease Center (PIADC) and Greg Weddell and Patricia Tanttila of Genentech for technical assistance. The work was greatly facilitated by the constant attendance and help of K.A. The dideoxy- sequencing was done by Richard Najarian. The oligonucleotides used in this project were synthesized by Mark Vasser, Parkash Jhurani, and Dr. Roberto Crea of Genentech. We thank Dr. J. S. Walker of PIADC's Biosafety Committee, Dr. G. Still of the USDA Science and Education Administration, Dr. H. Kryder of the USDA Vectors Committee, Dr. S. Barban of NIH-ORDA, and the NIH-RAC and FMD subcommittee for assistance, and Dr. J. J. Callis, director of PIADC, for his help and for his encouragement throughout this project.

1 September 1981; revised 19 October 1981

Regulation of Leucine Metabolism in Man: A Stable Isotope Study

Abstract. *Leucine catabolism is regulated by either of the first two degradative steps: (reversible) transamination to the keto acid or subsequent decarboxylation. A method is described to measure rates of leucine transamination, reamination, and keto acid oxidation. The method is applied directly to humans by infusing the nonradioactive tracer,* L-[^{15}*N,1-*^{13}*C]leucine. Leucine transamination was found to be operating several times faster than the keto acid decarboxylation and to be of equal magnitude in adult human males under two different dietary conditions, postabsorptive and fed. These results indicate that decarboxylation, not transamination, is the rate-limiting step in normal human leucine metabolism.*

The branched-chain amino acids leucine, valine, and isoleucine play a prominent role in the amino acid metabolism of muscle. In contrast to the other essential amino acids that are oxidized by the liver, the branched-chain amino acids are catabolized primarily by peripheral tissues such as muscle (*1*). This catabolism is thought to represent an important muscle energy source during early starvation and an important nitrogen source for muscle alanine and glutamine production for subsequent hepatic gluconeogenesis (*1*). Because of the unusual properties of the branched-chain amino acids, much research has focused on their metabolism, particularly the metabolism of leucine.

Control of leucine oxidation occurs at either or both of the first two steps of catabolism: transamination of the leucine to α-ketoisocaproate (KIC) or decarboxylation of KIC (Fig. 1). In muscle the latter step is thought to be rate controlling, although transamination activity also changes in response to various perturbations (*1*). Our knowledge of the control of leucine oxidation comes largely from studies with [^{14}C]leucine and perfused or isolated animal tissue systems. These systems can only approximate the physiology of the intact animal where multiple additional substrate and hormonal regulatory interactions are present. Moreover, species differences in leucine metabolism limit extrapolation of animal data to man.

Because the first step in leucine catabolism, transamination to KIC, is reversible (*2*), the use of a [^{14}C]leucine tracer alone supplies information on the generation of [^{14}C]KIC, but provides no insight into the rate of reamination of KIC to leucine. In this report we describe a method for measuring the rates of deamination, reamination, and oxidation of leucine in man using the safe, nonradioactive tracer L-[^{15}N,1-^{13}C]leucine.

During a primed, continuous infusion of L-[^{15}N,1-^{13}C]leucine, dilution of the dilabeled [^{15}N,1-^{13}C]leucine in plasma reflects the appearance of unlabeled leucine derived primarily from leucine release from protein breakdown and from dietary leucine intake. [^{15}N,1-^{13}C]Leucine is removed from the system by routes such as leucine incorporation into protein (protein synthesis) and leucine oxidation—the latter causes the differential release of the labels. Initial removal of ^{15}N by leucine transamination in the forward direction produces a [1-^{13}C]KIC (Fig. 1). The labeled keto acid has two fates: (i) decarboxylation to $^{13}CO_2$ or (ii) reamination to leucine, which produces singly labeled [1-^{13}C]leucine (*3*). Thus, mass spectrometric determination of the various labeled species present, [^{15}N,1-^{13}C]leucine, [1-^{13}C]leucine, and $^{13}CO_2$, allows solution of the overall model for leucine catabolism (Fig. 1).

The specific solution requires consideration of leucine carbon and nitrogen disposition. Figure 2 presents a model for leucine C oxidation (*4*). Leucine enters the free leucine pool by dietary intake (*I*) and leucine release from protein breakdown (*B*). Net leucine removal occurs by leucine incorporation into protein (*S*) and leucine oxidation (*C*). At steady state, leucine appearance will equal leucine disappearance which is net leucine C flux (Q_C):

$$Q_C = I + B = S + C \quad (1)$$

The leucine carboxyl-^{13}C label is not lost by leucine transamination to and from KIC, only by the subsequent decar-

Table 1. The effects of feeding and fasting on leucine metabolism measured with a primed, continuous infusion of [^{15}N,1-^{13}C]leucine. Data are given as means ± standard error for three subjects infused in the postabsorptive state and four subjects infused in the fed state.

Parameter	Value (μmole/kg-hour)	
	Postabsorptive	Fed
Net leucine C flux (Q_C)	83.9 ± 6.6	153.0 ± 7.5*
Leucine N flux (Q_N)	198.9 ± 23.2	273.4 ± 11.8†
Leucine oxidation (C)	10.6 ± 1.6	31.6 ± 3.2*
Leucine transamination to KIC (X_O)	121.8 ± 19.2	152.1 ± 10.9
KIC transamination to leucine (X_N)	111.2 ± 18.0	120.5 ± 8.6

*Difference between postabsorptive and fed states, $P < .005$. †$P < .05$.

Table 2. Relative values of leucine metabolism determined from data in Table 1.

Parameter	Postabsorptive	Fed
Percentage of leucine flux oxidized (C/Q_C)	11.9 ± 1.3	21.0 ± 2.5*
Percentage of KIC reaminated to leucine (X_N/X_O)	91.2 ± 0.8	79.2 ± 1.4†
Percentage of KIC oxidized (C/X_O)	8.8 ± 0.8	20.8 ± 1.4†

*Difference between postabsorptive and fed states, $P < .05$. †$P < .005$.

0036-8075/81/1204-1129$01.00/0

boxylation of the KIC. Therefore, the leucine C flux is a "net" flux because it contains the irreversible net leucine oxidation component. This is in contrast to the leucine N flux.

Leucine N also enters from the diet and is incorporated and released from protein (I, S, and B) at the same rate as the leucine carbon skeleton (Fig. 3). Because leucine N is lost by deamination (X_O) and returned by reamination of KIC (X_N), Eq. 1 is modified to reflect these additional processes:

$$Q_N = I + B + X_N = S + X_O \quad (2)$$

When the leucine N and C models are combined (Eq. 2 minus Eq. 1), then:

$$Q_N - Q_C = X_N = X_O - C \quad (3)$$

The difference between the leucine N and C fluxes ($Q_N - Q_C$), both measured from the dilution of the labeled tracer in plasma (*5*), is equal to the rate of leucine formation from KIC reamination (X_N). Since leucine decarboxylation (C), is measured from expired $^{13}CO_2$ release (*5*), the model can also be solved for the rate of leucine deamination (X_O).

It is important to remember that the apparent leucine N flux measured with dilabeled [^{15}N,1-^{13}C]leucine tracer may be considerably higher than a flux measured with monolabeled [^{15}N]leucine. Because transamination is reversible, a ^{15}N removed from a monolabeled [^{15}N]leucine may be placed back on a KIC via reamination. Thus, there is recycling of the ^{15}N label between leucine and the transaminating free N pool (Fig. 3). The more transamination is reversible

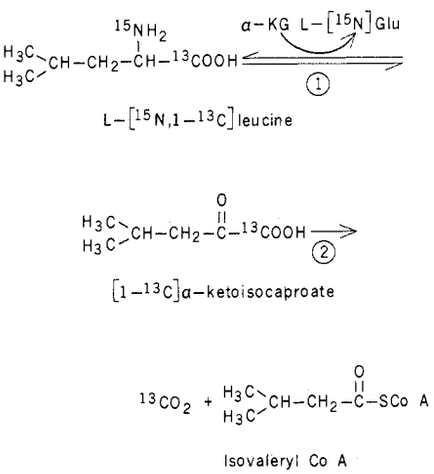

Fig. 1. Metabolism of L-[^{15}N,1-^{13}C]leucine. Step 1: transamination of leucine with α-ketoglutarate (α-KG) via leucine amino transferase (E.C. 2.6.1.6) (branched-chain amino acid transaminase); the ^{15}N label is removed and incorporated into a [^{15}N]glutamate. Step 2: decarboxylation of KIC via branched-chain ketoacid dehydrogenase (E.C. 1.2.4.4); the carboxyl-^{13}C is released as $^{13}CO_2$.

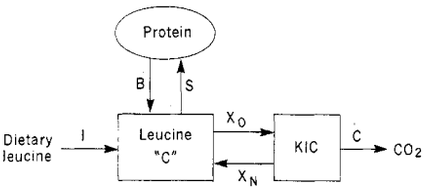

Fig. 2. Model for leucine metabolism in terms of the effects on the carboxyl carbon. The leucine carboxyl C enters the free leucine pool (leucine "C") via dietary intake (I) and protein breakdown (B) and leaves via incorporation into protein (S) and decarboxylation of KIC (C). Transamination of leucine to KIC (X_O) or of KIC to leucine (X_N) does not remove the carboxyl C from the system.

and rapid, the greater the underestimate in leucine N flux measured with a [^{15}N]leucine tracer. In contrast, the probability is much lower so that a ^{15}N will combine with a [1-^{13}C]KIC to reform a [^{15}N,1-^{13}C]leucine (*3*). The [^{15}N,1-^{13}C]leucine tracer discriminates against ^{15}N recycling and produces a higher, more realistic value for leucine N flux.

Leucine kinetics were measured in adult male subjects that were primed (*6*) and then infused continuously for 7 hours with L-[^{15}N,1-^{13}C]leucine. The subjects were tested under two different dietary conditions, postabsorptive and fed, in order to test the effect of feeding on the control of leucine catabolism. In the first set of studies, three healthy, normal weight, adult men were infused intravenously for 7 hours starting at 8:00 a.m. Blood and breath samples were collected throughout the infusion period for all the studies. The isotopic enrichment of plasma leucine was determined by chemical ionization gas chromatography–mass spectrometry (*7, 8*). Rates of leucine metabolism were computed from the data obtained at isotopic steady state.

Table 1 shows that in both the postabsorptive and fed states, Q_N was significantly faster than Q_C. This is because of the faster removal of ^{15}N by leucine transamination (X_O) compared to [1-^{13}C]KIC decarboxylation (C): 122 as opposed to 11 μmole/kg-hour in the postabsorptive state. Besides the absolute rate of transamination, the fractional rate of KIC reamination was considerably higher than the rate of KIC decarboxylation. In the postabsorptive state, 91 percent of the KIC formed was reaminated to leucine (X_N/X_O), as opposed to the 9 percent that continued on to be decarboxylated (C/X_O). These results demonstrate higher transamination rates than found in an earlier study (*9, 10*).

As we have shown (*5*), protein intake increases the leucine C flux. To compensate for the increased leucine intake, the body increases both the rate of leucine incorporation into body protein via protein synthesis and leucine oxidation (*5*). Is the leucine-intake–induced increase in oxidation due to a primary change in transamination, decarboxylation, or both? Although the rate of KIC decarboxylation increased significantly between the postabsorptive and fed states, transamination rates (X_O and X_N) changed insignificantly (Table 1). Furthermore, 21 percent of the KIC formed went on to decarboxylation in the fed state, compared with 9 percent in the postabsorptive state. This significant increase in the fraction of KIC continuing on to decarboxylation during feeding in the face of an insignificant change in the transamination rate shows that transamination was modified just enough to compensate for the increased rate of KIC decarboxylation, and that the decarboxylation step regulates human leucine oxidation.

These results affirm earlier work by others using animal tissue perfusion or homogenate systems (*1*). Those data demonstrated that in muscle the branched-chain amino acid transaminase is more active than the α-ketoacid dehydrogenase, but that in liver the situation is reversed. Because of the difficulty in measuring the dehydrogenase enzyme activity (*1, 11*), these earlier data are only qualitative. Furthermore, the tissue preparation systems do not necessarily reflect the relationships among all the body tissues. The data presented have shown that KIC decarboxylation is the regulating step for whole-body leucine oxidation. Muscle transaminates leucine and releases significant quantities of KIC, presumably for uptake and oxidation by liver (*1*). This implies that in both muscle and liver decarboxylation is limiting under normal physiological condi-

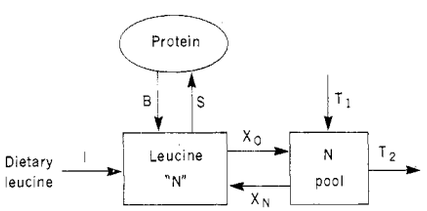

Fig. 3. Model for leucine metabolism in terms of the effects on the amino N. The leucine N enters the free leucine pool (leucine "N") via dietary intake (I), protein breakdown (B), and reamination of a KIC, where the N comes from the transaminating N pool—primarily glutamate N. The leucine N leaves the free leucine pool via incorporation into protein (S) and transamination of leucine (X_N). The transaminating N pool contains other entry and exit routes (T_1 and T_2).

tions. Our model, of course, does not allow dissection of the magnitude of individual organ contributions or delivery of substrate limitations to the organs; however, the measured, integrated body rates are useful for investigating various pathophysiological processes on leucine metabolism as a whole. Finally, the stable isotope tracers permit the use of this approach in humans of all ages, and this scheme, with the choice of the appropriate model, may be applied to other amino acids.

D. E. MATTHEWS
D. M. BIER
Metabolism Division, Departments of Medicine and *Pediatrics, Washington University School of Medicine, St. Louis, Missouri 63110*
M. J. RENNIE
R. H. T. EDWARDS
University College Hospital Medical School, London, England
D. HALLIDAY
Clinical Research Centre, Harrow, England
D. J. MILLWARD
G. A. CLUGSTON
London School of Hygiene and Tropical Medicine, London, England

References and Notes

1. S. A. Adibi, *Metabolism* **25**, 1287 (1976); R. A. Odessey and A. L. Goldberg, *Am. J. Physiol.* **233**, 1376 (1972); T. W. Chang and A. L. Goldberg, *J. Biol. Chem.* **253**, 3677 (1978); R. Odessey and A. L. Goldberg, *Biochem. J.* **178**, 475 (1979); S. M. Hutson, T. C. Cree, A. E. Harper, *J. Biol. Chem.* **253**, 8126 (1978); M. Walser and J. R. Williamson, Eds., *Metabolism and Clinical Implications of Branched Chain Amino and Ketoacids* (Elsevier/North-Holland, New York, 1981).
2. R. T. Taylor and W. T. Jenkins, *J. Biol. Chem.* **241**, 4396 (1966).
3. Some [^{15}N]leucine may be formed from the transamination of a KIC and [^{15}N]glutamate, but the probability of a ^{15}N from glutamate being incorporated back into a [1-^{13}C]KIC when it is reaminated to reform a [^{15}N,1-^{13}C]leucine is very low. Thus, transamination of [^{15}N,1-^{13}C]-leucine irreversibly removes the dilabeled leucine.
4. This model has been used previously with an L-[1-^{13}C]leucine tracer to measure the kinetic parameters Q_C, C, S, and B in Fig. 2 [see (*5*)].
5. D. E. Matthews, K. J. Motil, D. K. Rohrbaugh, J. F. Burke, V. R. Young, D. M. Bier, *Am. J. Physiol.* **238**, E473 (1980); K. J. Motil, D. E. Matthews, D. M. Bier, J. F. Burke, H. M. Munro, V. R. Young, *ibid.* **240**, E712 (1981).
6. The infusion protocol consisted of administering intravenously a priming dose of sodium [^{13}C]bicarbonate (90 percent ^{13}C) and L-[^{15}N,1-^{13}C]leucine (99 percent ^{15}N, 92 percent ^{13}C) (0.08 mg/kg and 7.5 μmole/kg, respectively), and then infusing intravenously for 7 hours L-[^{15}N,1-^{13}C]leucine at the rate of 7.5 μmole per kilogram of body weight per hour. The fed subjects also received 0.08 g of protein per kilogram per hour from hourly meals (about 180 ml of Ensure, a milk and soya protein mixture from Ross Labs).
7. Plasma di- and monolabeled leucine enrichments were determined by selected ion monitoring–chemical ionization–gas chromatography–mass spectrometry [see (*8*)]. The dilabeled [^{15}N,1-^{13}C]leucine species was measured from the 218/216 molecular ion intensity ratio. Monolabeled leucine (either [^{15}N]leucine or [1-^{13}C]leucine) was measured from the 217/216 molecular ion intensity ratio. Total leucine ^{15}N enrichment (both [^{15}N,1-^{13}C]leucine and [^{15}N]leucine) was determined from the 129/128 fragment ion intensity ratio [the fragment does not contain the carboxyl-C; see (*8*)]. Total leucine ^{13}C enrichment (both [^{15}N,1-^{13}C]leucine and [1-^{13}C]leucine) was calculated from the three above-measured values. The dilabeled [^{15}N,1-^{13}C]leucine enrichment was used to calculate leucine N flux; the total leucine ^{13}C enrichment was used to calculate leucine C flux.
8. D. E. Matthews, E. Ben-Galim, D. M. Bier, *Anal. Chem.* **51**, 80 (1979).
9. In our first infusion studies [see (*10*)], the infused, commercially obtained L-[^{15}N,1-^{13}C]leucine was later found to contain D-[^{15}N,1-^{13}C]leucine as well. Thus, the previously reported leucine N flux values were underestimated.
10. D. E. Matthews, M. J. Rennie, D. Halliday, D. J. Millward, G. C. Clugston, R. H. T. Edwards, D. M. Bier, in *Metabolism and Clinical Implications of Branched Chain Amino and Ketoacids*, M. Walser and J. R. Williamson, Eds. (Elsevier/North-Holland, New York, 1981), pp. 313–316.
11. R. M. Wohlhueter and A. E. Harper, *J. Biol. Chem.* **245**, 2391 (1970); P. J. Parker and F. J. Randle, *FEBS Lett.* **112**, 186 (1980).
12. This work was supported by NIH grants AM-25994, HD-10667, and RR-00954, the National Livestock and Meat Board, the Medical Research Council of England, and the Wellcome Trust.

11 May 1981; revised 23 July 1981

Caterpillar Setae: Insulation for an Ectotherm

Abstract. *Gypsy moth caterpillars have long, soft setae distributed along the lateral portions of the body, but only short, stiff setae on the dorsal surface. Setae act as selective insulation for caterpillars by reducing the rates of convective heat exchange without affecting the rates of radiative heat exchange. Changes in posture abolish the effects of the setae by maximizing convection and minimizing radiant heat uptake.*

The importance of insulation to the heat balance of endotherms is well documented. It serves either as a means of conserving body heat (*1*) or as a radiation shield to prevent excessive radiant heating (*2*). Since insulation retards rates of heat exchange between the body and the environment, it would appear to be useless to small ectotherms, which must obtain all of their heat from the environment.

Although they are ectothermic, caterpillars routinely exhibit body temperatures far in excess of the air temperature (*3*) and are capable of thermoregulation by altering radiative and convective heat exchange through postural changes and movements in response to different microclimates (*4*). The present study demonstrates that insulation is significant to the thermal balance of gypsy moth caterpillars and that it differs in appearance and function from that of endotherms.

Late-instar gypsy moth (*Lymantria dispar*) caterpillars were supplied by the New Jersey Department of Agriculture Plant Pest Laboratory. The caterpillars, maintained in small plastic cups at room temperature, were fed a synthetic diet.

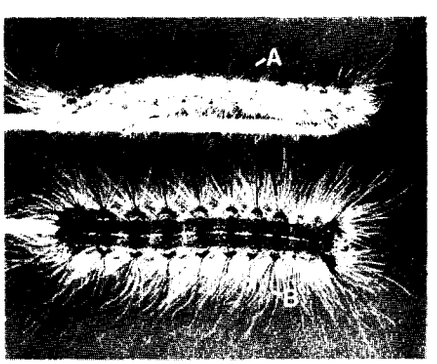

Fig. 1. Distribution of setae on gypsy moth caterpillars. (A) Short, stiff, spinelike setae on dorsal surface. (B) Long, soft setae in addition to short, stiff setae on lateral portion of the body.

Cooling curves for live and dead caterpillars in still air and at wind speeds of 1.0 and 2.0 m/sec were measured by suspending the caterpillars in a small wind tunnel (*5*). Before being placed in the wind tunnel, the caterpillars were heated to approximately 40°C with an incandescent light. They were then placed inside the tunnel and allowed to cool.

The effect of radiant heating on body temperature was measured by attaching caterpillars, with thermocouples inserted into the rectum, to wooden dowels (diameter, 2 mm) and exposing them to radiant heat loads (*6*) of 350, 700, and 975 W/m^2 from a 5000 K color temperature photoflood lamp (Kodak, FAY 650W).

Setae were removed from the caterpillars with forceps or jewelers' pliers. The setae were easily removed, and the caterpillars appeared to be unharmed by the procedure. Several caterpillars with setae removed pupated successfully and emerged into normal adults.

To determine the magnitude of heat loss by evaporation, we measured evaporative water loss of dead caterpillars with and without setae by weighing them before and after a 1-hour exposure at 35°C in dry air.

Setae occur in tufts, arising from setal stalks on tubercles located in distinct regions of each body segment (*7*). Two distinct types of setae occur, and different types do not always occur in the same location. Only short (mean length, 2.9 mm; $N = 29$), stiff setae arise from the dorsal tubercles (Fig. 1A). The largest outcropping of setae arise from the

0036-8075/81/1204-1131S01.00/0